

# Colorimetric/ratio fluorescence determination of glucose using bifunctional carbon dots

Yuan Chunling, Yao Xiaotiao, Xu Yuanjin, Qin Xiu, Shi Rui, Cheng Shiqi, Wang Yilin

theanalyst@163.com

(Guangxi Key Laboratory of electrochemical energy materials, School of chemistry and chemical engineering, Guangxi University, Nanning 530004)

## Abstract:

Based on biomass (taro leaf). Iron was prepared by hydrothermal method with ammonium ferric sulfate dodecahydrate and urea as raw materials. Nitrogen Co doped carbon dots (Fe, N-CDs) were characterized by transmission electron microscopy and X-ray photoelectron spectroscopy. The Fe, N-CDs not only has peroxidase like activity, but also can produce strong fluorescence emission at 450 nm. Using Fe, N-CDs and o-phenylenediamine (OPD) as probes, a dual signal colorimetric/ratio fluorescence method for the determination of hydrogen peroxide ( $H_2O_2$ ) was established. In the presence of  $H_2O_2$ , Fe, N-CDs catalyze the oxidation of OPD to yellow 2, 3-diaminophenazine (DAP), which has a characteristic absorption peak at 420 nm. Under the excitation of 360 nm wavelength light, DAP has strong fluorescence emission at 550 nm; DAP can quench the fluorescence of Fe and N-CDs at 450 nm due to the fluorescence internal filtering effect. Based on this, the absorbance of DAP at 420 nm ( $A_{420}$ ) and the fluorescence intensity ratio of DAP to Fe, N-CDs ( $I_{550}/I_{450}$ ) can be used for the quantitative analysis of  $H_2O_2$ . Considering that glucose oxidase can catalyze the oxidation of glucose to  $H_2O_2$ , a colorimetric/ratio fluorescence dual signal glucose determination method was further developed. Under the conditions of pH=5.4, temperature 40°C, 1.75 mmol/L OPD and reaction time 25 min, when the glucose concentration is in the range of 1.0~100 $\mu$ mol/L, the values of  $A_{420}$  and  $I_{550}/I_{450}$  have a good linear relationship with the concentration, and the detection limits of the method are respectively 0.8 (colorimetry) and 0.6  $\mu$ mol/L (ratio fluorescence). The method was successfully applied to the determination of glucose in human serum.

**Keywords:** carbon point; colorimetry; ratio fluorescence; glucose; determination

Chinese library classification number: O657.3

Document mark code A

Glucose is the main energy source and metabolic intermediate in biological

---

Received on: January 8, 2021. Online publishing date: April 7, 2021

Fund Project: National Natural Science Foundation of China (approval No.: 61664002) and Guangxi Graduate Education Innovation Program (approval No.: Ycsw2020016).

Contact profile: Wang Yilin, male, doctor, Professor, mainly engaged in chemical biosensor research. E-mail: [theanalyst@163.com](mailto:theanalyst@163.com)

activities, and plays an important role in the process of life. Abnormal blood glucose level is usually considered to be related to diabetes. Hypoglycemia, metabolic disorders and other diseases [1, 2]. Therefore, rapid and accurate determination of glucose concentration in serum is of great significance for disease diagnosis. At present, chromatographic analysis [3, 4]. Detection techniques such as electrical analysis [5, 6] and optical analysis [7, 8] have been applied to the determination of glucose. Because of its fast response. With the advantages of low cost and high sensitivity, colorimetric and fluorescent light analysis techniques have attracted much attention [7]. With the continuous development of nanotechnology, various nano materials have been widely used in the field of optical analysis. Some metal oxides [9]. Metal sulfide [10] and noble metal [11] nano materials are used for colorimetric determination of glucose because they have peroxidase like properties and can catalyze the oxidation of 3, 3', 5, 5' - tetramethylbenzidine (TMB) by  $H_2O_2$ . Due to the large absorption spectrum bandwidth and molar absorption coefficient,  $mno_2$  nanosheets can effectively quench rare earth nanoparticles ( $NaYF_4:YB$ ,  $Tm@NaYF_4$  The fluorescence of nanoparticles [12] and copper nanoclusters [13]; the addition of  $H_2O_2$  can reduce  $mno_2$  to Mn and restore the quenched fluorescence. Combined with the principle that glucose oxidase catalyzes the oxidation of glucose to  $H_2O_2$ , the above nano materials have been used to construct "off-on" fluorescent probes for the determination of glucose concentration. So far, there are many reports on the determination of glucose by colorimetry or fluorescence, but few reports on the simultaneous determination of glucose by these two methods [14, 15]. Studies [14, 15] showed that  $znfe_2o_4$  magnetic microspheres. Pd nanoparticles can catalyze the oxidation of o-phenylenediamine (OPD) by  $H_2O_2$  to produce fluorescent yellow product 2, 3-diaminophenazine (DAP); the presence of DAP will lead to boron and nitrogen Co doped carbon dots (B, N-CDs). Fluorescence quenching of  $C_3N_4$  nanosheets. Accordingly, Li<sup>[14]</sup> and Qiu<sup>[15]</sup> research groups have developed a new dual signal glucose determination method based on colorimetry and ratio fluorescence, both of which use two nano (or micron) materials.

Compared with other nano materials, cds has the advantages of simple preparation. High stability. Good biocompatibility and strong luminous ability [16]. As peroxidase like or fluorescent nano materials, cds are widely used in biochemical analysis, cell imaging and other research fields [17~22], but there are few reports of bifunctional cds with peroxidase like activity and fluorescence emission characteristics [23~25]. Cds prepared from biomass materials such as *Azadirachta indica* leaves [23] and mustard seeds [24] can not only emit fluorescence, but also catalyze the oxidation of TMB by  $H_2O_2$ . However, relevant studies only apply its catalytic function to the determination of  $H_2O_2$  and ascorbic acid; bifunctional iron can be prepared by using organic amine and ferric nitrate as reactants. Nitrogen Co doped cds, which can be used for colorimetric/ratio fluorescence determination of xanthine [25]. Element doping can not only improve the fluorescence quantum yield of cds, but also change the internal electronic environment of cds, endow cds with new functions and expand its application fields [26]. Based on the key role of iron in peroxidase and the fact that nitrogen doping

can improve the fluorescence characteristics of cds, this paper takes biomass (taro leaf). Iron was prepared by hydrothermal method with ammonium ferric sulfate dodecahydrate and urea as starting materials. Nitrogen Co doped cds (Fe, N-CDs), the obtained Fe, N-CDs not only has peroxidase like activity, but also can produce strong fluorescence emission at 450 nm (Figure 1). Based on the bifunctional properties of Fe, N-CDs, a colorimetric/ratio fluorescence method for the determination of glucose concentration was established and successfully applied to the analysis of actual samples.

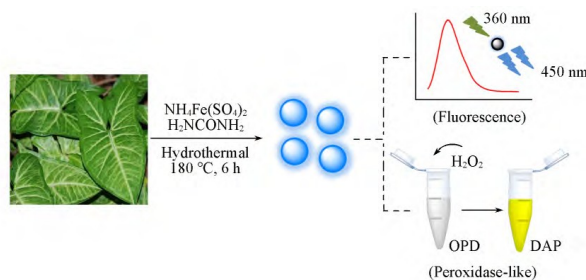


**Figure 1 Preparation and properties of Fe, N-cds**

## 1 Experimental part

### 1.1 Reagents and instruments

Ammonium ferric sulfate dodecahydrate [ $\text{NH}_4\text{Fe}(\text{SO}_4)_2 \cdot 12\text{H}_2\text{O}$ ]. Urea ( $\text{n}_2\text{hconh}_2$ ). Sodium acetate trihydrate. Glacial acetic acid and hydrogen peroxide (Guangdong Guanghua Technology Co., Ltd.); glucose. Phenylalanine. Glycine. Isoleucine. Threonine. Aspartic acid. Valine. Tryptophan and serine (Tianjin Damao Chemical Reagent Factory); O-phenylenediamine (OPD, Shanghai Aladdin Reagent Co., Ltd.); glucose oxidase (Beijing sulaibao Technology Co., Ltd.). All reagents used are analytically pure, and the experimental water is deionized water.

RF-5301PC fluorescence spectrophotometer (Shimadzu company of Japan); uv<sup>-</sup>4802 UV visible spectrophotometer (Shanghai longnico company); TECNAI G2 F20 S-Twin transmission electron microscope (Fei company of the United States); Nicolet IS5 Fourier transform infrared spectrometer (Thermo Fisher, USA); FLS1000 fluorescence spectrometer (Edinburgh company, UK)

### 1.2 Preparation of Fe, N-CDs

Wash the taro leaves, dry the wet water on the surface, and then cut them into pieces. Weigh 2.0 g and put them in a 75mL reactor. Add 0.8 g  $\text{NH}_4\text{Fe}(\text{SO}_4)_2 \cdot 12\text{H}_2\text{O}$ , 0.2 g  $\text{N}_2\text{HCONH}_2$  and 25mL deionized water, mix them evenly and seal them; place the reaction kettle in a  $180\text{ }^\circ\text{C}$  constant temperature drying oven for 6 hours. After natural cooling to room temperature, filter with funnel to obtain dark brown solution; reuse  $0.22\mu\text{m}$  microfiltration membrane removes large particle aggregates in the solution; dialysis the reaction solution for 24 hours to remove unreacted reagents, collect the solution in the bag and dilute it to 25 mL, and store it in a  $4\text{ }^\circ\text{C}$  refrigerator for standby.

### 1.3 Determination of H<sub>2</sub>O<sub>2</sub> and glucose

Determination of H<sub>2</sub>O<sub>2</sub>: add 0.5 mL of H<sub>2</sub>O<sub>2</sub> solutions with different concentrations into a series of colorimetric tubes. 0.5 mL of 17.5 mmol/L OPD solution and 100 μL Fe, N-CDs solution, after mixing evenly, dilute to 5.0 mL with HAC naac (0.2 mol/L) buffer solution with pH=5.4, and place it in a 40°C water bath for 25 minutes. The absorption spectra were scanned in the range of 330~550 nm, and the fluorescence spectra were recorded under the excitation of 360 nm wavelength light. The experiments were carried out in parallel for 3 times.

Determination of glucose: add 0.5 mL of 10 mmol/L NaH<sub>2</sub>PO<sub>4</sub>-Na<sub>2</sub>HPO (4 pH=7.0) buffer solution successively into a series of colorimetric tubes. 0.5 mL of glucose solution with different concentrations and 0.1 mL of 2.0 mg/mL glucose oxidase were mixed evenly and incubated in a 37°C water bath for 30 minutes to produce H<sub>2</sub>O<sub>2</sub>; then, add 0.5 mL of 17.5 mmol/L OPD solution and 100 μL Fe, N-CDs solution, dilute to 5.0 mL with 0.2 mol/L HAc-NaAc buffer solution (pH =5.4), mix evenly, and the subsequent process is the same as the determination of H<sub>2</sub>O<sub>2</sub>. The experiment is carried out in parallel for 3 times.

## 2 Results and discussion

### 2.1 Characterization of Fe, N-CDs

The morphology and particle size of Fe, N-CDs were characterized by transmission electron microscope (TEM). It can be seen from Figure 2 (a) that Fe and N-CDs are approximately spherical and have good dispersion; clear lattice stripes with a spacing of 0.23 nm can be seen from the high-resolution transmission electron microscope photos (illustration), which correspond to the graphene (100) surface [27]. According to the analysis of nano measurer software [Figure 2 (b)], the particle size of Fe and N-CDs is mainly distributed in the range of 1.34~3.68 nm, and the average particle size is about 2.51 nm

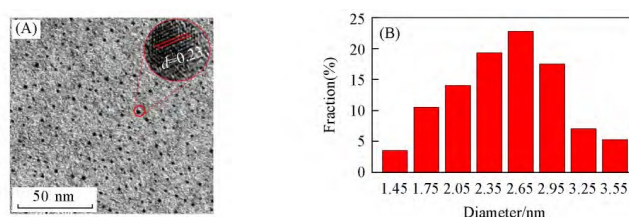


**Figure 2 TEM image(A) and particle size distribution diagram(B) of Fe, N-cds Inset of(A) is the relative HRTEM image.**

Under the irradiation of 365 nm UV lamp, Fe, N-CDs emit bright blue fluorescence [Figure 3 (a) illustration]. When the excitation wavelength increased from 310 nm to 440 nm, the fluorescence emission peak of Fe, N-CDs red shifted from 427 nm to 472 nm; the fluorescence intensity increased first and then decreased; when excited by light with a wavelength of 360 nm, the fluorescence emission is the strongest [Figure 3 (a)]. This excitation dependent emission behavior is related to the surface defects and particle size of particles [27] Fe, N-CDs solution has strong light absorption

in the UV region, and the absorption peak at 270 nm is attributed to the  $\pi - \pi^*$  transition of C=C or C=N [28] (see supporting information Figure S<sub>1</sub> in this paper). Fourier transform infrared spectroscopy (FTIR) was used to analyze the groups contained in Fe, N-CDs [Figure 3 (b)]. The wide peak at 3150  $\text{cm}^{-1}$  was attributed to the stretching vibration of O-H and N-H, the peak at 1630  $\text{cm}^{-1}$  was attributed to the stretching vibration of C=O and C=C, and the peak at 1400 and 1120  $\text{cm}^{-1}$  was attributed to the stretching vibration of C-OH and C-O-C, respectively. FTIR analysis showed that there were hydrophilic groups -COOH, -OH and -NH<sub>2</sub> on the surface of Fe, N-CDs, which made them have good water solubility.

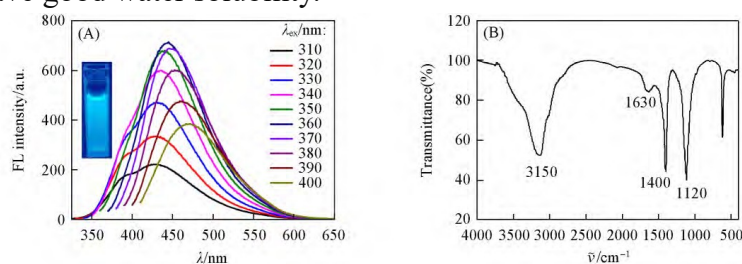


**Figure 3 Emission spectra of Fe, N-cds excited at 310–440 Nm(A) and FTIR spectrum of Fe, N-cds(B)**

The elemental composition and functional groups of Fe and N-CDs were characterized by X-ray photoelectron spectroscopy (XPS). It can be seen from the full scan spectrum (Figure 4) that cds is mainly composed of carbon (44.02%). Nitrogen (13.41%). The binding energies of oxygen (39.98%) and iron (2.59%) are 284.8401.3531.5 and 710.7 EV, respectively The high-resolution XPS spectrum of C<sub>1s</sub> contains three peaks of 284.7286.1 and 288.3 EV, corresponding to C=C, C=O and O-C=O functional groups respectively. [29] The high-resolution XPS spectrum of N<sub>1s</sub> shows two peaks of 399.8 and 401.5 EV, corresponding to C-N-C and N-H functional groups respectively. [30] There are 531.3 and 532.4 EV peaks in the high-resolution XPS spectrum of O<sub>1s</sub>, which belong to C-OH/C-O-C and C=O bond respectively. [31] The Fe<sub>2p</sub> spectrum contains four peaks of 710.7, 714.1, 724.7 and 727.6 EV, corresponding to Fe<sub>2p<sub>3/2</sub></sub><sup>2+</sup>, Fe<sub>2p<sub>3/2</sub></sub><sup>3+</sup>, Fe<sub>2p<sub>1/2</sub></sub><sup>2+</sup> and Fe<sub>2p<sub>1/2</sub></sub><sup>2+</sup> [32] respectively [See the supporting information Figure S<sub>2</sub> (A)~(D)]. The above results show that Fe and n elements have indeed been doped into cds; the surface of Fe, N-CDs is rich in O-containing and N-containing functional groups.

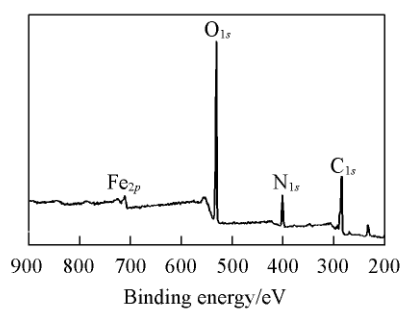


**Figure 4 Survey spectrum of Fe, N-cds**

## 2.2 Catalytic activity of Fe, N-CDs and mechanism of glucose double signal determination

In order to study the peroxidase like activity of Fe, N-CDs, a control experiment was carried out in HAC naac buffer solution with  $\text{pH}=5.4$ . The solution containing Fe, N-CDs and OPD is colorless, and there is no absorption peak in the UV Vis Spectrum [Figure 5 (a) line a]; the solution containing  $\text{H}_2\text{O}_2$  and OPD has a weak absorption peak at 420 nm [Figure 5 (a) spectral line b], and its solution is light yellow, indicating that  $\text{H}_2\text{O}_2$  can slowly oxidize OPD to DAP; when Fe and N-CDs are present, the solution containing  $\text{H}_2\text{O}_2$  and OPD has a strong absorption peak at 420 nm [Figure 5 (a) spectral line c], and its solution is dark yellow. The above data show that Fe, N-CDs have peroxidase like activity and can catalyze the oxidation of OPD by  $\text{H}_2\text{O}_2$ .

DAP solution is yellow, and its absorption peak is at 420 nm; under the excitation of 360 nm wavelength light, the fluorescence emission peak of Fe, N-CDs is located at 450 nm. It can be seen from Figure 5 (b) that the absorption spectrum of DAP overlaps greatly with the fluorescence spectrum of Fe, N-CDs; when the two coexist, the fluorescence quenching of Fe, N-CDs can be caused by fluorescence internal filtration effect (IFE) or fluorescence resonance energy transfer (Fref). Before and after the addition of Fe, N-CDs, the position and absorption intensity of DAP absorption peak are almost unchanged [see the supporting information Figure S<sub>3</sub> (a)], indicating that there is no complex between Fe, N-CDs and DAP, that is, FRET between Fe, N-CDs and DAP is impossible [33]. In addition, before and after adding DAP, the fluorescence lifetime of Fe, N-CDs did not change significantly [see the supporting information Figure S<sub>3</sub> (b)], indicating that there was no charge transfer between Fe, N-CDs and DAP, so the fluorescence quenching of Fe, N-CDs was not caused by charge transfer [14]. Therefore, when the two coexist, the fluorescence quenching of Fe, N-CDs is caused by IFE.

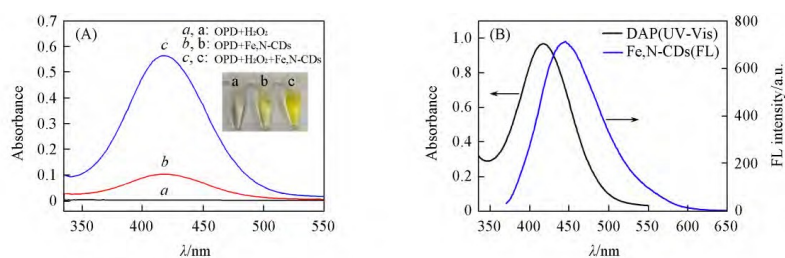


**Figure 5 Absorbance spectra of different solutions in 0.2 mol/L HAc-NaAc buffer solution at  $\text{pH}=5.4$ (A) and absorbance spectrum of DAP and emission spectrum of Fe,N-CDs(B)**

Inset of (A) shows the corresponding photograph.

Fe, N-CDs can catalyze  $\text{H}_2\text{O}_2$  to oxidize OPD to produce DAP; excited by 360nm wavelength light, DAP has a fluorescence emission peak at 550 nm, while Fe, N-CDs also have a fluorescence emission peak at 450 nm under the excitation of the same wavelength light; DAP quenches the fluorescence of Fe, N-CDs through IFE. That is, adding  $\text{H}_2\text{O}_2$  to Fe, N-CDs/opd system will not only change the color of the solution, but also change the relative fluorescence intensity of DAP and Fe, N-CDs; with the increase of  $\text{H}_2\text{O}_2$  concentration, the absorbance of DAP at 420 nm and the fluorescence

intensity at 550 nm increased, while the fluorescence intensity of Fe and N-CDs at 450 nm decreased. The concentration of H<sub>2</sub>O<sub>2</sub> can be determined by measuring the absorbance of DAP at 420 nm and the fluorescence intensity ratio of DAP to Fe, N-CDs ( $I_{550}/I_{450}$ ); H<sub>2</sub>O<sub>2</sub> is one of the products of glucose oxidation catalyzed by glucose oxidase. Based on this, a colorimetric/ratio fluorescence dual signal glucose determination method can be further established (Figure 6)

### 2.3 Optimization of experimental conditions

In order to obtain the best signal response, pH was investigated with the relative fluorescence intensity  $I_{550}/I_{450}$  (where  $I_{550}$  and  $I_{450}$  represent the fluorescence emission intensity at 550 and 450 nm, respectively). Temperature. Effects of reaction time and OPD concentration on the oxidation of OPD by H<sub>2</sub>O<sub>2</sub> catalyzed by Fe, N-CQDs. Considering that peroxidase like enzymes usually show strong catalytic activity under weak acidic conditions, the effect of medium acidity on  $I_{550}/I_{450}$  was investigated in the pH range of 5.0~6.2 with HAC naac buffer as the medium. It can be seen from Figure S<sub>4</sub> (a) (see the supporting information in this article) that with the increase of ph, the value of  $I_{550}/I_{450}$  shows a change law of first increasing and then decreasing, and when ph=5.4, the value of  $I_{550}/I_{450}$  is the largest. Therefore, the experiment was carried out in HAC naac buffer with ph=5.4. At room temperature, the oxidation rate of OPD catalyzed by Fe, N-CDs is slow, and the color change of the reaction system is not obvious. Figure S<sub>4</sub> (b) (see the supporting information in this article) shows the relationship between the measured I value and temperature change of Fe, N-CDs/H<sub>2</sub>O<sub>2</sub>/opd mixture after incubation in a 30~60°C water bath. It can be seen that 40°C is a relatively suitable temperature. With the extension of the reaction time, the value of I also increases, and it is basically stable at 25 min [see the supporting information Figure S<sub>4</sub> (C)]. In order to ensure the maximum fluorescence ratio and stable signal response, 25 min is selected as the best reaction time. With the increase of OPD concentration, the  $I_{550}/I_{450}$  value gradually increases, and when the concentration is 1.75 mmol/L, the  $I_{550}/I_{450}$  value tends to be stable [see the supporting information Figure S<sub>4</sub> (d)]. The final selected experimental conditions are pH=5.4, temperature 40°C, reaction time 25 min, 1.75 mmol/L OPD.

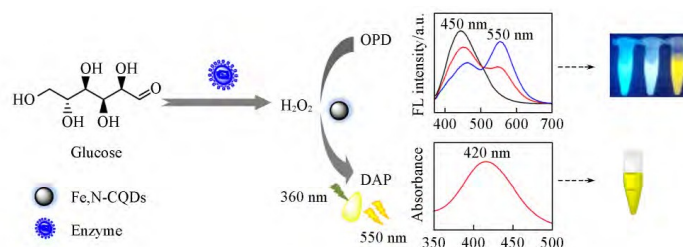


Figure 6 Schematic diagram of detection principle

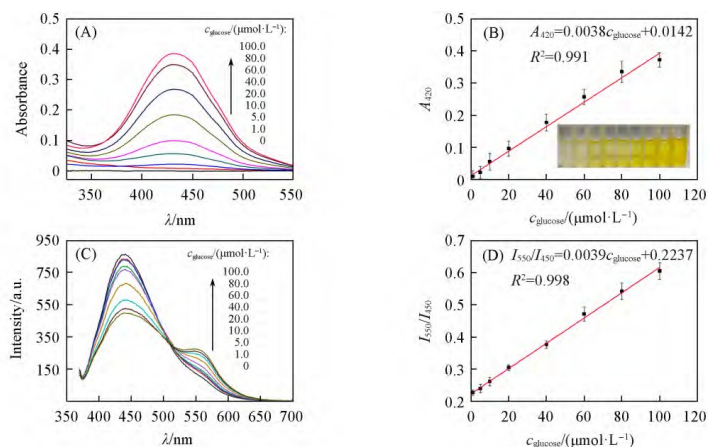
### 2.4 Colorimetric/ratio fluorescence dual signal detection of H<sub>2</sub>O<sub>2</sub> And glucose

Under the optimized conditions, the effect of H<sub>2</sub>O<sub>2</sub> concentration on the absorption and fluorescence spectra of the system was investigated. The results of UV-Vis

absorption spectrum showed that when the concentration of H<sub>2</sub>O<sub>2</sub> increased from 1.0 μmol/L increased to 300 μmol/L, the wavelength of the characteristic absorption peak of DAP at 420 nm remains unchanged, and the absorption intensity gradually increases [see the supporting information Figure S5 (A)]; and the absorbance value ( $A_{420}$ ) at 420 nm has a good linear relationship with H<sub>2</sub>O<sub>2</sub> concentration [see the supporting information Figure S5(B)]. The linear equation is  $A_{420} = 0.0039c_{\text{H}_2\text{O}_2} + 0.0087$ , and the correlation coefficient is 0.996. The fluorescence measurement results show that with the increase of H<sub>2</sub>O<sub>2</sub> concentration, the fluorescence of DAP at 550 nm gradually increases, while the fluorescence of Fe, N-CQDs at 450 nm gradually decreases [see the supporting information Figure S5(C)] H<sub>2</sub>O<sub>2</sub> concentration is within the range of 1.0~80 μmol/L, there is a good linear relationship between  $I_{550}/I_{450}$  value and H<sub>2</sub>O<sub>2</sub> concentration [see the supporting information Figure S5(D)], the linear equation is  $I_{550} / I_{450} = 0.0039c_{\text{H}_2\text{O}_2} + 0.2606$ , and the correlation coefficient is 0.998. Detection limit of colorimetric and ratio fluorimetry ( $3\sigma/k$ ) are respectively 0.7 and 0.6 μmol/L, indicating that the method has high sensitivity.

Glucose will produce H<sub>2</sub>O<sub>2</sub> after catalytic oxidation by glucose oxidase. Therefore, a dual signal method for the determination of glucose can be further established. Figure 7 (a) shows the absorption spectrum of DAP depending on glucose concentration. With the increase of glucose concentration, the absorbance at 420 nm gradually increased; within the concentration range of 1.0 and 100 μmol/L, the absorbance of DAP has a good linear relationship with glucose concentration [Figure 7 (B)], and the regression equation is  $A_{420} = 0.0038c_{\text{glucose}} + 0.0142$  ( $R^2 = 0.991$ ). As can be seen from Figure 7 (C), with the increase of glucose concentration, the fluorescence intensity of DAP at 550 nm increases, while the fluorescence intensity of Fe, N-CDs at 450 nm decreases; between 1.0 and 100 μmol/L concentration,  $I_{550}/I_{450}$  value is directly proportional to glucose concentration [Figure 7 (d)], and the regression equation is  $I_{550} / I_{450} = 0.0039c_{\text{glucose}} + 0.2237$  ( $R^2 = 0.998$ ). The detection limits of colorimetry and ratio fluorescence were respectively 0.8 and 0.6 μmol/L, indicating that the method has high sensitivity. The linear range and detection limit of the method are superior to or comparable to the reported methods (Table 1); and the color of the final test solution deepens with the increase of glucose concentration [Figure 7 (b) illustration], and the lowest concentration that can be distinguished by naked eyes is 5.0 μmol/L, this method can realize the visual detection of low concentration glucose.





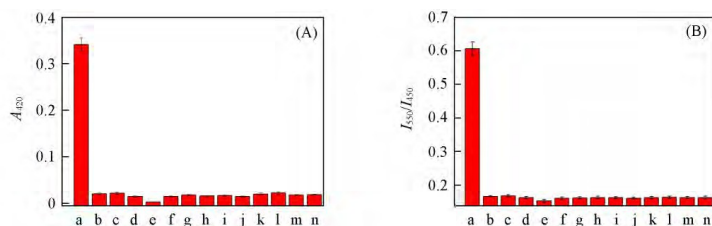
**Figure 7** Absorption(A) and emission(C) spectra of Fe, N-cds-OPD with different concentrations of glucose, linear relationship between  $A_{420}$  And glucose concentration(B) and linear relationship between  $I_{550}/I_{450}$  and glucose concentration(D) Inset of(B) is the photograph of the solutions corresponding to(A).

Table 1 Comparison of different methods for detecting glucose

Method	Material	Linear range( $\mu\text{mol}\cdot\text{L}^{-1}$ )	LOD( $\mu\text{mol}\cdot\text{L}^{-1}$ )	Ref.
Chromatography	3-OMG	0.39-25	0.39	[4]
Electrochemical	$\text{Dy}_2(\text{MoO}_4)_3\text{-AuNPs}$	10-1000	3.33	[5]
Fluorimetry	$\text{Tm@NaYF}_4$ Nanoparticles	0-250	3.7	[12]
Fluorimetry	Co-NC	1-50	0.15	[34]
Colorimetry	$\text{mFe}_2\text{O}_3\text{-G}$	0.5-10	0.5	[35]
Colorimetry	$\text{MoS}_2$	5-150	1.2	[10]
Fluorimetry	Fe, N-CDs	1.0-100	0.6	This work
Colorimetry	Fe, N-CDs	1.0-100	0.8	This work

## 2.5 Method selectivity

To evaluate the selectivity of the method, common metal ions in serum such as  $\text{Na}^+$ ,  $\text{K}^+$ ,  $\text{Mg}^{2+}$ ,  $\text{Zn}^{2+}$  and a series of amino acids [phenylalanine (PHE)] were selected. Glycine (Gly). Isoleucine (ILE). Threonine (THR). Aspartic acid (ASP). Tryptophan (TRP). Valine (VAL) and serine (SER)] were cultivated as distractors instead of glucose. After color development, the absorption and fluorescence signals were measured respectively. Figure 8 (a) and (b) respectively show the colorimetric and ratio fluorescence responses when the concentration of glucose (Glu) is 0.1 mmol/L and the concentration of each interfering substance is 1.0 mmol/L. Although the concentration of each interfering substance is 10 times that of glucose, only glucose can cause significant changes in the two analytical signals, which is related to the high selectivity of glucose oxidase. Therefore, the selectivity of this method is good.



**Figure 8 Selectivities of colorimetric(A) and ratio fluorescence for glucose detection(B)**

The concentration of glucose was 0.1 Mmol/L, of other substances was 1.0 Mmol/L. A. Glu; b. Blank; c. Na<sup>+</sup>; d. K<sup>+</sup>; e. Zn<sup>2+</sup>; f. Mg<sup>2+</sup>; g. Phe; h. Glycine; i. Ile; j. Thr; k. Asp; l. Try; m. Val; n. Ser.

## 2.6 Actual sample analysis

In order to verify the feasibility of the method, the content of glucose in human serum was determined. Take 0.8mL of serum sample, add 0.8mL of trichloroacetic acid (mass fraction 5%), and centrifuge for 10 minutes at the speed of 10000 r/min to remove serum protein. Add 0.1mL of treated serum and different concentrations of glucose to the reaction system, and determine according to the steps in Section 1.3. The results are shown in Table 2. The colorimetric values of glucose concentration in the sample detection solution were respectively 40.2 and 35.9  $\mu\text{mol/L}$ , according to the dilution ratio, the concentration of glucose in the original sample is calculated to be 4.02 and 3.59 mmol/L respectively, which is basically consistent with the clinical measurement results (4.53 and 3.86 mmol/L), both within the normal range. In addition, the results of colorimetry and ratio fluorescence are consistent; the recovery rate is 93.3% - 111.5%; the RSD is between 0.4% and 6.8%, indicating that the method has high accuracy and precision, and can be applied to the analysis of actual samples.

Table 2 Detection of glucose in human serum\*

Sample/ ( $\mu\text{mol}\cdot\text{L}^{-1}$ )	Added 1)	Colorimetric(%)			Ratiometric fluorescence		
		Found/ ( $\mu\text{mol}\cdot\text{L}^{-1}$ )	Recovery (%)	RSD ( $n=3$ , %)	Found ( $\mu\text{mol}\cdot\text{L}^{-1}$ )	Recovery (%)	RSD ( $n=3$ , %)
Serum 1	0	40.2	—	1.5	39.1	—	0.4
	20	61.5	106.5	2.9	61.4	111.5	3.0
	40	82.3	105.2	3.7	80.0	102.2	3.1
Serum 2	0	35.9	—	3.3	35.3	—	2.1
	20	57.6	108.5	1.4	55.2	99.5	4.6
	40	78.3	106.0	5.2	72.6	93.3	6.8

\* The serum was diluted 100 Times.

## 3 Conclusion

Take biomass (leaves of syncarpic taro). Bifunctional Fe, N-CDs with peroxidase like activity and fluorescence characteristics were prepared from iron and nitrogen-containing substances. After adding H<sub>2</sub>O<sub>2</sub> to the mixed solution of Fe, N-CDs and OPD,

Fe, N-CDs can catalyze  $H_2O_2$  to oxidize OPD to produce DAP that can emit fluorescence. DAP and Fe, N-CDs form a double emission system. The relative fluorescence intensity of the system and the absorbance of DAP are regulated by the concentration of  $H_2O_2$ . Based on the principle that glucose oxidase catalyzes the oxidation of glucose to produce  $H_2O_2$ , a colorimetric/ratio fluorescence dual signal analytical method for the determination of glucose was developed. This method has high sensitivity. It has been applied to the determination of glucose in human serum, and the results are consistent with the clinical values. Compared with the reported double signal glucose determination method, this method only needs to prepare a nano material.

For supporting information, see <http://www.Cjcu.Jlu.Edu.Cn/CN/10.7503/cjcu20210019>.

## References

- [1] Zhang J. L., Dai X., Song Z. L., Han R., Ma L. Z., Fan G. C., Luo X. L., *Sens. Actuators B Chem.*, 2020, 304, 127304
- [2] Baek S. H., Roh J., Park C. Y., Kim M. W., Shi R., Kailasa S. K., Park T. J., *Mat. Sci. Eng. C-Mater.* 2020, 107, 110273
- [3] Xie W. Q., Gong Y. X., Yu K. X., *J. Chromatogr. A*, 2017, 1520143–146
- [4] Ling Z. L., Xu P., Zhong Z. Y., Wang F., Shu N., Zhang J., Tang X. G., Liu L., Liu X. D., *Biomed. Chromatogr.*, 2016, 30(4), 601–605
- [5] Huang H. P., Yue Y. F., Xu L., Lü L. L., Hu Y. M., *Chem. J. Chinese Universities*, 2017, 38(4), 554–560
- [6] Xu L., Lin Y. Q., Chen X., Lu Y. L., Yang W. S., *Chem. J. Chinese Universities*, 2016, 37(3), 442–447
- [7] Liu T., Zhang S. X., Liu W., Zhao S., Lu Z. W., Wang Y. Y., Wang G. T., Zou P., Wang X. X., Zhao Q. B., Rao H. B., *Sens. Actuators B Chem.*, 2020, 305, 127524
- [8] Rashtbari S., Dehghan G., Amini M., *Anal. Chim. Acta*, 2020, 1110, 98–108
- [9] Cheng X. W., Huang L., Yang X. Y., Elzatahry A. A., Alghamdi A., Deng Y. H., *J. Colloid Interf. Sci.*, 2019, 535, 425–435
- [10] Lin T. R., Zhong L. S., Guo L. Q., Fu F. F., Chen G. N., *Nanoscale*, 2014, 6, 11856–11862
- [11] Liu H., Hua Y., Cai Y. Y., Feng L. P., Li S., Wang H., *Anal. Chim. Acta*, 2019, 1092, 57–65
- [12] Yuan J., Cen Y., Kong X. J., Wu S., Liu C. L., Yu R. Q., Chu X., *ACS Appl. Mater. Interfaces*, 2015, 7, 10548–10555
- [13] Wang H. B., Chen Y., Li N., Lin Y. M., *Microchim. Acta*, 2017, 184, 515–523
- [14] Xiao N., Liu S. G., Mo S., Yang Y. Z., Han L., Ju Y. J., Li N. B., Luo H. Q., *Sens. Actuators B Chem.*, 2015, 273, 1735–1743
- [15] Zhang W. C., Li X., Xu X. C., He Y. F., Qiu F. X., Pan J. M., Niu X. H., *J. Mater. Chem. B*, 2019, 7, 223–239
- [16] Wang C. K., Tan R., Li L. B., Liu D., *Chem. Res. Chinese Universities*, 2019, 35(5), 767–774

- [17] Zhong Q. M., Huang X. H., Qin Q. M., Su A. M., Chen Y. Y., Liu X. Y., Wang Y. L., *Chinese J. Anal. Chem.*, 2018, 46(7), 1062–1068
- [18] Geng X., Sun Y. Q., Li Z. H., Yang R., Zhao Y. M., Guo Y. F., Xu J. J., Li F. T., Wang Y., Lu S. Y., Qu L. B. *Small*, 2019, 15, 1901517
- [19] Guo S., Sun Y. Q., Geng X., Yang R., Xiao L. H., Qu L. B., Li Z. H., *J. Mater. Chem. B*, 2020, 8, 736–742
- [20] Chen Y. Y., Qin X., Yuan C. L., Shi R., Wang Y. L., *Dyes and Pigments*, 2020, 181, 108529
- [21] Su A. M., Wang D., Shu X., Zhong Q. M., Chen Y. R., Liu J. C., Wang Y. L., *Chem. Res. Chinese Universities*, 2018, 34(2), 164–168
- [22] Yuan C. L., Qin X., Xu Y. J., Jing Q. Q., Shi R., Wang Y. L., *Microchem. J.*, 2020, 159, 105365
- [23] Yadav P. K., Singh V. K., Chandra S., Bano D., Kumar V., Talat M., Hasan S. H., *ACS Biomater. Sci. Eng.*, 2019, 5, 623–632
- [24] Chandra S., Singh V. K., Yadav P. K., Bano D., Kumar V., Pandey V. K., Talat M., Hasan S. H., *Anal. Chim. Acta*, 2019, 1054, 145–156
- [25] Wang L. Z., Liu Y., Yang Z. P., Wang Y. Y., Rao H. B., Yue G. Z., Wu C. M., Lu C. F., Wang X. X., *Dyes and Pigments*, 2020, 180, 108486
- [26] Zhuo S. J., Guan Y. Y., Hui L., Fang J., Zhang P., Du J. Y., *Analyst*, 2019, 144, 656–662
- [27] Hu Y. F., Zhang L. L., Li X. F., Liu R. J., Lin L. Y., Zhao S. L., *ACS Sustainable Chem. Eng.*, 2017, 5, 4992–5000
- [28] Sun X. H., He J., Yang S. H., Zheng M. D., Wang Y. Y., Ma S., Zheng H. P., *J. Photoch. Photobio. B*, 2017, 175, 219–225
- [29] Shen J., Shang S. M., Chen X. Y., Wang D., Cai Y., *Mat. Sci. Eng. C-Mater.* 2017, 76, 856–864
- [30] Gu D., Shang S. M., Yu, Q., Shen J., *Appl. Surf. Sci.*, 2016, 390, 38–42
- [31] Wen X. P., Shi L. H., Wen G. M., Li Y. Y., Dong C., Yang J., Shuang S. M., *Sens. Actuators B Chem.*, 2015, 221, 769–776
- [32] Yang W. Q., Huang T. T., Zhao M. M., Luo F., Weng W., Wei Q. H., Lin Z. Y., Chen G. N., *Talanta*, 2017, 164, 1–6
- [33] Fang A. J., Long Q., Wu Q. Q., Li H. T., Zhang Y. Y., Yao S. Z., *Talanta*, 2016, 148, 129–134
- [34] Qian P. C., Qin Y. N., Lyu Y., L., Li Y., F., Wang L., Wang S., Liu Y. Q., *Anal. Bioanal. Chem.* 2019, 411, 1517–1524
- [35] Xing Z. C., Tian J. Q., Asiri A. M., Qusti A. H., Al-Youbi A. O., Sun X. P., *Biosens. Bioelectron.*, 2014, 52, 452–457